I&EC research
Industrial & Engineering Chemistry Research

Article

Cite This: Ind. Eng. Chem. Res. 2017, 56, 13133-13145

pubs.acs.org/IECR

Kinetics of Methanol Synthesis from Carbon Dioxide Hydrogenation over Copper−Zinc Oxide Catalysts

Jean-François Portha,*[,†,‡] Ksenia Parkhomenko,[§] Kilian Kobl,[§] Anne-Cécile Roger,[§] Sofiane Arab,[∥] Jean-Marc Commenge,[†,‡] and Laurent Falk[†,‡]

[†]Laboratoire Réactions et Génie des Procédés, UMR 7274, Université de Lorraine, 1 rue Grandville, F-54000 Nancy, France

[‡]Laboratoire Réactions et Génie des Procédés, UMR 7274, CNRS, 1 rue Grandville, F-54000 Nancy, France

[§]Institut de Chimie et Procédés pour l'Energie, l'Environnement et la Santé, UMR 7515 CNRS-Université de Strasbourg, 25 rue Becquerel, 67087 Strasbourg Cedex 2, France

[∥]IFP Energies Nouvelles, Rond-point de l'échangeur de Solaize, BP 3, 69360 Solaize, France

Supporting Information

ABSTRACT: Kinetics of methanol synthesis from carbon dioxide hydrogenation is studied on two noncommercial catalysts: a copper−zinc oxide catalyst on alumina (CuZA) and a copper−zinc oxide catalyst on zirconia (CuZZ). The experiments have been performed in an isothermal fixed bed reactor with a temperature range between 200 and 230 °C, a total pressure comprised between 50 and 80 bar, a gas hourly space velocity (GSHV) between 7800 and 23 400 h^{-1} and for different hydrogen:carbon dioxide molar ratios (between 2 and 6). Unlike other works in the literature, no carbon monoxide is contained in the feed which corresponds to the conditions of some recent industrial applications, the influence of the catalyst support has been tested to improve the methanol selectivity. The experimental data were modeled using the kinetic laws and adsorption coefficients determined by Graaf et al. based on a Langmuir−Hinshelwood−Hougen−Watson (LHHW) mechanism. The reactor model was based on an isothermal pseudo-homogeneous plug flow model without mass-transfer limitations. An optimization procedure was performed in order to identify new kinetic parameters. A good agreement between experimental data and modeling results was highlighted.

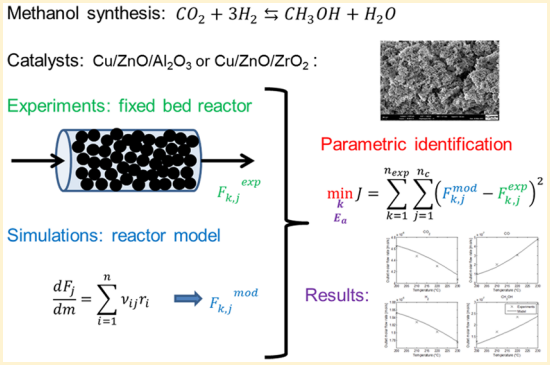

1. INTRODUCTION

The concentration increase of greenhouse gases in the atmosphere is a crucial subject that mankind must address. The potential consequences are climatic changes such as global warming. The conversion of carbon dioxide, which is the main greenhouse gas, to a high-value-added chemical may be a good solution to limit the global warming. Moreover, the synthesis of a chemical is interesting to store energy from renewable but intermittent sources (wind power or photovoltaic panels for instance) or from excess nuclear power on the electric grid. It has been shown[1] that methanol is a very important chemical, because it is a key intermediate to produce formaldehyde, amines, acetic acid, esters, or alternative fuels such as dimethyl ether (DME), and methanol can be generated from CO_2. Several methods for the efficient reductive conversion of CO_2 to methanol exist, including bireforming with methane, catalytic hydrogenation, and electrochemical conversion.[2] A review focusing specifically on the catalytic carbon dioxide hydrogenation to methanol and describing catalytic features, reaction pathways, and recent technological progress has been written by Jadhav et al.[3] The catalytic methanol synthesis requires a large amount of hydrogen. This hydrogen can be produced by the electrolysis of water supplied with the excess of energy on the electric grid, meaning that methanol is a solution to store energy. Consequently, the flow rate of the produced hydrogen will not be constant and the methanol synthesis process will need to withstand flow variations and operate under transient conditions.

Methanol production from carbon dioxide is achieved through a catalytic process in the gas phase, according to the following reversible reactions: the carbon monoxide hydrogenation (reaction 1), the reverse water-gas shift (RWGS) reaction (reaction 2), and the carbon dioxide hydrogenation (reaction 3).

$$CO + 2H_2 \leftrightarrows CH_3OH \qquad \Delta_r H°(298\ K) = -90.5\ kJ/mol \tag{1}$$

$$CO_2 + H_2 \rightleftarrows CO + H_2O \qquad \Delta_r H°(298\ K) = 41.1\ kJ/mol \tag{2}$$

Special Issue: Tapio Salmi Festschrift

Received: April 5, 2017
Revised: July 5, 2017
Accepted: July 5, 2017
Published: July 5, 2017

DOI: 10.1021/acs.iecr.7b01323
Ind. Eng. Chem. Res. 2017, 56, 13133−13145

$$CO_2 + 3H_2 \leftrightarrows CH_3OH + H_2O$$
$$\Delta_r H°(298\ K) = -49.4\ kJ/mol \quad (3)$$

The desired reaction is obviously the carbon dioxide hydrogenation, which occurs in parallel to the RWGS reaction. As carbon monoxide is produced through the RWGS, the carbon monoxide reaction is also taken into account. Some side reactions can occur, especially methanation or dehydration of the formed methanol to produce DME. The occurrence of these reactions is minimized by the selectivity of the used catalyst and the choice of the operating conditions. They are not considered in this work.

Reaction 3 is a linear combination of reactions 1 and 2. Then, of course, reaction 3 should not be taken into account to perform a thermodynamic equilibrium calculation. Nevertheless, to establish a kinetic model, authors have often considered the three previously cited reactions, which must also be taken into account to perform a sizing of a chemical reactor. Reactions 1 and 3 are exothermic reactions that require a trade-off temperature to maximize conversion by taking into account kinetic and thermodynamic constraints. Currently, methanol synthesis is achieved on an industrial scale via a cooled multitubular packed-bed reactor working at high pressure (between 50 bar and 80 bar) and moderate temperature (between 200 °C and 300 °C) enclosed by a shell.[4] The pressure on the shell side, where the cooling fluid is boiling demineralized water under pressure, enables one to control the temperature profile of the reaction via water phase change. Since the methanol synthesis is a reaction whose conversion is limited by thermodynamic equilibrium, the recycling of unconverted reactants is necessary. To avoid the accumulation of inert gases in the recycled stream, a purge system is also required. If the level of inert gases (nitrogen and methane in the conditions of the methanol synthesis) increases in the feed, the purge and recycle ratios also increase, which implies a loss of chemicals and an increase in the capital cost (larger compressors and reactors) and in the operational cost (compression power).[5] Note that the hydrogen contained in the purge could be recovered by a membrane separation unit, a cryogenic distillation unit, or a pressure swing adsorption unit. One way to characterize the reaction is using the parameter M, defined from molar fractions at the reactor inlet (eq 4):

$$M = \frac{y_{H_2} - y_{CO_2}}{y_{CO} + y_{CO_2}} \quad (4)$$

For a stoichiometric $CO/CO_2/H_2$ mixture, the parameter M has a value of 2. A value larger than 2 indicates a mixture rich in H_2, and reciprocally. Therefore, a syngas composition with a stoichiometric number M slightly above 2 is the optimum for methanol synthesis.[6] Several technologies are available for the synthesis of methanol from syngas: for example, Air Liquide offers a large-scale technology called the "Lurgi MegaMethanol" process. Besides, studies have also tested the synthesis of methanol at industrial scale from carbon dioxide over a commercially available catalyst.[7]

In this work, a brief literature review is performed to report the kinetic schemes and the corresponding rate laws that enable to represent the methanol synthesis. The preparation and characterization of two catalysts ($Cu/ZnO/Al_2O_3$ and $Cu/ZnO/ZrO_2$), together with the experiments realized for the catalytic tests, are also described. The experiments have been performed in an isothermal fixed bed reactor with a temperature range between 200 °C and 230 °C, a total pressure comprised between 50 bar and 80 bar, a gas hourly space velocity (GHSV) between 7800 h^{-1} and 23 400 h^{-1} and for different hydrogen:carbon dioxide molar ratios (between 2 and 6). An identification of kinetic parameters is carried out by considering a pseudo-homogenous reactor model, taking into account the kinetic model based on a Langmuir−Hinshelwood−Hougen−Watson (LHHW) mechanism developed by Graaf et al.[8−10] The results are finally discussed. The objective is to determine a set of optimized kinetic parameters that enable one to size an industrial and delocalized reactor with reliability. The distinctive features of the work are observed at three levels. First, although methanol synthesis from syngas ($CO/CO_2/H_2$ mixture) is known for a long time, the hydrogenation of pure CO_2 to produce methanol has been less studied. Second, the influence of the catalyst support is tested: although Al_2O_3 is classically used for syngas hydrogenation, ZrO_2 is used here to convert pure CO_2 into methanol; the selectivity of methanol is assumed to be optimized this way. Third, both catalysts have been tested under relatively large operating conditions (temperature, pressure, feed composition, and GHSV) in order to support potential variation of feed composition or of inlet pressure. Moreover, the range of operating conditions can be different from those used in previous works: for instance, the pressure range is different compared to the conditions used in the study of Graaf et al.[9] To the best knowledge of the authors, no kinetic parameters based on a LHHW mechanism have been optimized under these operating conditions for the $Cu/ZnO/ZrO_2$ catalyst with a pure CO_2/H_2 mix as feed.

2. KINETIC STUDIES ABOUT METHANOL SYNTHESIS: A LITERATURE REVIEW

Several kinetic models have been reported in the literature to describe the methanol synthesis. The studies vary in reaction conditions (temperature and pressure), feedstock composition and used catalysts. Some models are derived for the methanol synthesis from CO and H_2, while some others take CO_2 into consideration in the feed. Different forms of the kinetic laws are obtained and are dependent on the rate-determining step that is considered in the mechanism.

First, two recent and interesting studies focusing on microkinetic aspects can be cited. The work of Grabow and Mavrikakis[11] describes a microkinetic model, with 49 elementary steps, and presents the different intermediates involved in the methanol synthesis. An interesting result is that, under typical conditions, 2/3 of the methanol is produced from CO_2 hydrogenation. As concluded by the authors themselves, further studies are needed to determine more-quantitative results. As stated in the paper of Kunkes et al.,[12] one of the major mechanistic questions is related to whether methanol synthesis and RWGS are parallel pathways, methanol synthesis and RWGS share a common intermediate, or methanol formation proceeds by sequential RWGS and CO hydrogenation. Both last hypotheses are clearly excluded in the conclusion of this study.

Then, some studies concerning macrokinetic models with explicit rate laws are reviewed. Graaf et al.[8−10] have developed a kinetic model based on an LHHW mechanism, taking into account the involved reactions (reactions 1, 2, and 3) over a commercial $CuO/ZnO/Al_2O_3$ MK-101 Haldor Topsoe catalyst. The determined rate laws are based on a dual-site Langmuir−Hinshelwood mechanism (competitive adsorption of CO and CO_2 on a metallic copper site and competitive adsorption of H_2 and H_2O on a ZnO site) with dissociative hydrogen adsorption

DOI: 10.1021/acs.iecr.7b01323
Ind. Eng. Chem. Res. 2017, 56, 13133−13145

for temperatures between 210 and 275 °C and pressures between 15 and 50 bar.

Van den Bussche and Froment[13] have established a kinetic model taking into account only the water gas-shift reaction (reaction 2) and the carbon dioxide hydrogenation (reaction 3). The model couples the rate of both overall reactions by taking into account a surface oxygen intermediate. The authors assume that CO_2, previously obtained by the WGS reaction, is the main source of carbon in methanol synthesis and a dissociative adsorption of H_2 and CO_2 is the rate-determining step. The experiments were performed over a commercial $CuO/ZnO/Al_2O_3$ catalyst from Imperial Chemical Industries (ICI 51−2). The temperature ranges between 180 °C and 280 °C, the total pressure was between 15 bar and 51 bar, and the CO/CO_2 molar ratio was between 0 and 4.1.

Park et al.[14] have proposed a kinetic model based on a LHHW mechanism that takes into account the three reversible reactions (reactions 1, 2, and 3) over a commercial $Cu/ZnO/Al_2O_3$ catalyst (MegaMax 700, Süd-Chemie). They addressed the development of a kinetic model based on three-site adsorption (Cu^{1+}, Cu^0, ZnO). Indeed, detailed elementary steps for both CO and CO_2 hydrogenation based on two-site adsorption[9] were modified, considering an additional adsorption site for CO_2 with dissociative hydrogen adsorption, leading to kinetic laws close to those obtained by Graaf et al.[9] The temperature ranges between 220 °C and 340 °C and pressure between 50 bar and 90 bar.

In the work of Askgaard et al.,[15] the kinetic model used is based on another kinetic model that was developed initially for the water gas-shift reaction.[16] The power law model taking into account the thermodynamic equilibrium is developed considering 16 elementary steps. If the agreement between measured and model-predicted rates is good, there is no argument that enables one to conclude that this model is better than the one developed by Graaf et al.[9]

Other kinetic models have been developed.[17,18] By testing these kinetic expressions in a pseudo-homogeneous model representing an adiabatic plug flow reactor (with an inlet temperature and pressure fixed to 250 °C and 80 bar, respectively), the obtained temperature profile shows that the thermodynamic equilibrium is not reached at the reactor outlet.[6] These two models are not considered in the present work

Table 1 summarizes some kinetic studies for the methanol synthesis.

Experimental studies show, when both CO and CO_2 are present, that CO_2 is the main source of methanol under usual conditions over $Cu/ZnO/Al_2O_3$ catalysts.[19] CO participates in the synthesis but after being converted into CO_2 by the water gas-shift reaction. At high space velocities, methanol yield increases continuously as an increasing amount of CO is replaced by CO_2 (if CO_2 is the primary source of methanol, CO cannot be converted to CO_2 without water). At low space velocities, methanol yield shows a sharp increase, reaches a maximum and then decreases due to an inhibition of the active sites by water adsorption.

All models considered in Table 1 have been developed especially for CO-rich gas, which does not correspond to the present case study that mainly consists of CO_2 hydrogenation. Moreover, numerous studies have been performed at relatively low pressure. A new identification of the kinetic parameters, based on kinetic expressions provided in the literature is also required. Therefore, the kinetic laws derived by Graaf et al.[9] are considered when using pure CO_2 feedstock and high pressure (50−80 bar) for its hydrogenation to methanol.

Table 1. Kinetic Studies in the Literature for Methanol Synthesis

references	catalyst	reactants	range of temperature and pressure	reactions considered for parameter identification	feed composition (mol %)
Graaf et al.[9,10]	$Cu/Zn/Al_2O_3$ (Haldor Topsoe MK-101)	$CO/CO_2/H_2$	210−275 °C, 15−50 bar	1, 2, and 3	CO, 0−22; CO_2, 2−26; H_2, 67.4−90
Van den Bussche and Froment[13]	$Cu/ZnO/Al_2O_3$ (Imperial Chemical Industries, ICI 51−2)	$CO/CO_2/H_2$	180−280 °C, 15−51 bar	2 and 3	CO, 0−30; CO_2, 0−30; H_2: 70
Park et al.[14]	$Cu/ZnO/Al_2O_3$ (MegaMax 700, Süd-Chemie)	$CO/CO_2/H_2$	220−340 °C; 50−90 bar	1, 2, and 3	CO, 0−32; CO_2, 0−24; H_2, 50−83
Skrzypek et al.[17]	$CuO/ZnO/Al_2O_3$ (Blasiak)	$CO/CO_2/H_2$	187−277 °C, 30−90 bar	2 and 3	CO, 0−20; CO_2, 5−35; H_2, 10−80
Villa et al.[18]	$Cu/ZnO/Al_2O_3$	$CO/CO_2/H_2$	473−543 °C	1 and 2	

DOI: 10.1021/acs.iecr.7b01323
Ind. Eng. Chem. Res. 2017, 56, 13133−13145

3. EXPERIMENTAL SECTION

3.a. Catalyst Preparation and Characterization. Two interesting reviews have been reported about the catalyst features for the CO_2 hydrogenation to methanol. A detailed description of the efficiency of the active phase and the interactions with the support (such as ZrO_2) was reported by Liu et al.[20] It has been underlined that the preparation method has an important impact on the performance. Since 2003, a particular focus on catalysts based on Cu, Zn, alumina, and zirconia has been realized by Jadhav et al.[3] The incorporation of promoters such as Pd or Ga enables one to enhance the methanol yield.

In this work, catalysts, each containing 30 wt % of copper metal, $Cu/ZnO/Al_2O_3$ (CuZA) and $Cu/ZnO/ZrO_2$ (CuZZ), were prepared by coprecipitation of nitrate solutions of their respective metals with Na_2CO_3 solution. The details of the preparation method are described in a previous work.[21]

Specific surface areas measurements were performed by nitrogen adsorption−desorption at −196 °C using the Brunauer−Emmett−Teller (BET) method on a Micromeritics ASAP 2420 apparatus. Samples were previously outgassed at 250 °C for 3 h to remove adsorbed moisture. The metallic copper surface areas of the catalysts were measured by the N_2O reactive frontal chromatography method using a MicromeriticsAuto-Chem II analyzer with a TCD detector at a total flow rate of 50 mL_{SATP} min^{-1}. After reduction of 0.4 g of the sample at 280 °C, with a ramp of 1 °C min^{-1}, isotherm for 12 h under 10% H_2/Ar flow, followed by a purge with Ar, N_2O chemisorption was carried out at 50 °C under a 2% N_2O/Ar flow.[22]

Both tested catalysts have the same active phase: 30 wt % Cu^0 (37.5% CuO) and 41 wt % ZnO. They only differ in their support: the support corresponds to alumina for the CuZA catalyst and to zirconia for the CuZZ catalyst. After the synthesis, the catalysts were sieved to obtain a fraction of 50−125 μm, which was used for characterization and catalytic tests.

The CuZZ catalyst has an apparent density that is three times higher than that of the CuZA sample. It may be due to the morphology of the sample CuZZ and, especially, to the more-compact organization of the slits inside a particle as mentioned for the analysis of the specific surface area and porosity. Because of the difference in apparent density of the materials, the CuZZ catalyst was diluted in SiC to obtain the same catalytic bed volume. Other properties of the catalysts and the catalytic bed are given in Table 2. Appendix A in the Supporting Information explains, in more detail, the characterization techniques used to determine properties given in Table 2.

3.b. Reaction Setup and Catalytic Tests. The catalytic tests were carried out in a stainless steel reaction setup. The external diameter of the stainless steel tubular reactor is 1.27 cm, and the internal diameter is 1.01 cm. The properties of the catalytic bed are summarized in Table 3. A gas mixture bottle (molar composition: 31.5% CO_2, 63.5% H_2, and 5% N_2) was purchased from Air Liquide. Gas bottles of pure H_2, N_2, and Ar were purchased from Air Liquide and SOL France. Gas flows of the mixture bottle, of pure H_2, N_2, and Ar were regulated by Brooks SLA 5850S mass flow controllers connected to Brooks 0254 secondary electronics. Pressure was controlled by a Brooks 5866 back pressure regulator. The catalyst bed was placed between two pieces of quartz wool retained by a quartz tube and a metallic grid with gas flows pointing downward. The reactor was heated with an electrical THERMOCOAX heating element that was isolated with a quartz wool layer outside of the reactor. Temperature was regulated by a PID controller with a regulation thermocouple touching the catalyst bed inside the reactor at the effluent side. Liquid products (methanol and water) were trapped during the reaction in a first trap at room temperature and afterward in a second, water-cooled trap at 15 °C and analyzed offline using an Agilent 6890N gas chromatograph equipped with a SGE Solgelwax column and FID detector. Gases CO_2, CO, H_2, N_2, and Ar were analyzed online once per hour by an Inficon 3000 microchromatograph equipped with Molsieve 5 Å and Poraplot Q columns and TCD detectors. No traces of methane or other hydrocarbons, dimethyl ether, or alcohols other than methanol were detected, which justify the fact that side reactions are considered to be negligible.

The catalytic tests were carried out using the CuZA or CuZZ catalysts powders, which were sieved to a 50−125 μm particle fraction. The mass of catalyst was fixed to 135 mg in order to obtain a GHSV of 7800 h^{-1}, and the CuZZ catalyst was diluted in 387 mg of SiC in order to obtain the same catalytic bed volume of 0.307 cm^3. The following procedure was used for the experiments: the catalyst was reduced under H_2 flow (6.4 mL_{SATP} min^{-1}) at atmospheric pressure and by increasing the temperature (ramp from room temperature to 280 °C, using a rate of 1 °C min^{-1}, isotherm for 12 h). The reduced catalyst was then cooled to 100 °C under the same flow. The desired reaction gas flow rates were adjusted to a total volumetric flow rate of 40 mL_{SATP} min^{-1} and verified using an Agilent ADM 1000 flow meter. The reactor then was pressurized to the desired total pressure under reaction flow and the gas-phase composition was allowed to stabilize. The temperature was ramped at 1 °C min^{-1} to the desired reaction temperature. The moment when this temperature was reached was defined as the starting point of the reaction. The liquid phase was recovered at the end of each test in pressurized detachable traps and weighted, and its composition was analyzed. The reaction conditions and the results of catalytic tests for the CuZA catalyst are summarized in Table 4. The reaction conditions and the results of catalytic tests for the CuZZ catalyst are summarized in Table 5. Experimental results were checked for heat and mass-transfer limitations and no such limitations were found. Each data point that was taken into account for the parametric identification has been obtained after 50 h to ensure that catalyst aging does not falsify the results. All

Table 2. Catalyst Properties

property	CuZA	CuZZ
support type	Al_2O_3	ZrO_2
apparent density (g cm^{-3})	0.44	1.51
particle size (μm)	50−125	50−125
BET surface area (m^2 g^{-1})	110	62
average pore diameter (nm)	18	11
Cu^0 specific surface area (m^2 g^{-1})	9.6	8.3
reducibility (%)	102	99
porosity (cm^3 g^{-1})	0.51	0.16
catalyst tortuosity	7	

Table 3. Bed Properties

property	value
catalyst mass (mg)	135
bed volume (cm^3)	0.307
bed height (cm)	0.382
internal reactor diameter (cm)	1.01
bed porosity	0.41

DOI: 10.1021/acs.iecr.7b01323
Ind. Eng. Chem. Res. 2017, 56, 13133−13145

Table 4. Overview of Reaction Conditions and Results of Catalytic Tests over CuZA

				Inlet Partial Pressure (bar)					X (%)		S (%)	
exp	GHSV (h^{-1})	P (bar)	T (°C)	H_2	CO_2	N_2	Ar	H_2/CO_2 ratio	CO_2	H_2	MeOH	CO
A	7800	50	200	34.9	8.9	6.2	0.0	3.9	4.6	2.4	56	44
B	7800	50	210	34.9	8.9	6.2	0.0	3.9	7.7	3.4	45	55
C	7800	50	220	34.9	8.9	6.2	0.0	3.9	11.1	4.8	43	57
D	7800	50	230	34.9	8.9	6.2	0.0	3.9	15.8	6.3	38	62
1	7800	50	210	12.7	6.2	6.2	24.8	2.0	5.1	2.9	20	80
2	7800	50	210	18.8	6.2	6.2	18.7	3.0	5.9	3.1	33	67
3	7800	50	210	24.4	6.2	6.2	13.1	3.9	7.2	3.1	39	61
4	7800	50	210	31.3	6.2	6.2	6.3	5.0	9.3	3.2	42	58
5	7800	50	210	37.5	6.2	6.2	0.0	6.0	9.9	3.4	48	52
6	7800	50	210	24.4	12.0	6.2	7.4	2.0	4.8	3.9	37	63
7	7800	50	210	24.4	8.1	6.2	11.3	3.0	6.1	3.3	38	62
8	7800	50	210	24.4	4.9	6.2	14.5	5.0	8.8	2.9	38	62
9	7800	50	210	24.4	4.1	6.2	15.3	6.0	9.8	2.7	40	60
3a	7800	65	210	31.7	8.1	8.1	17.1	3.9	8.6	4.4	48	52
3b	7800	80	210	39.0	10.0	10.0	21.0	3.9	9.9	5.3	51	49
3.1	11700	50	210	24.4	6.3	6.3	13.1	3.9	5.6	2.6	39	61
3.2	23400	50	210	24.4	6.3	6.3	13.1	3.9	2.8	1.4	46	54

Table 5. Overview of Reaction Conditions and Results of Catalytic Tests over CuZZ

				Inlet Partial Pressure (bar)					X (%)		S (%)	
exp	GHSV (h^{-1})	P (bar)	T (°C)	H_2	CO_2	N_2	Ar	H_2/CO_2 ratio	CO_2	H_2	MeOH	CO
A	7800	50	200	34.9	8.9	6.2	0.0	3.9	3.9	2.5	70	30
B	7800	50	210	34.9	8.9	6.2	0.0	3.9	5.7	3.5	63	37
C	7800	50	220	34.9	8.9	6.2	0.0	3.9	8.7	4.7	56	44
D	7800	50	230	34.9	8.9	6.2	0.0	3.9	11.8	6.0	47	53
2	7800	50	220	18.8	6.2	6.2	18.7	3.0	6.1	3.5	36	64
4	7800	50	220	31.3	6.2	6.2	6.3	5.0	8.4	3.4	49	51
5	7800	50	220	37.5	6.2	6.2	0.0	6.0	10.0	3.7	55	45
6	7800	50	220	24.4	12.0	6.2	7.4	2.0	4.9	4.0	37	63
7	7800	50	220	24.4	8.1	6.2	11.3	3.0	6.5	3.9	39	61
8	7800	50	220	24.4	4.9	6.2	14.5	5.0	9.4	3.5	40	60

the details of data treatment are discussed in a previous work.[23] For the calculations of conversions and selectivities given in Tables 4 and 5, the molar amount of each substance integrated over the entire duration of the experiment was used. The expressions of CO_2 and H_2 conversions are given in eqs 5.

$$X_{CO_2} = \frac{n_{CH_3OH} + n_{CO}}{n_{CO_2,in}}$$

$$X_{H_2} = \frac{2n_{CH_3OH} + n_{H_2O}}{n_{H_2,in}} \quad (5)$$

The expressions of methanol and CO selectivities are given in eqs 6.

$$S_{CH_3OH} = \frac{n_{CH_3OH}}{n_{CH_3OH} + n_{CO}}$$

$$S_{CO} = 1 - S_{CH_3OH} \quad (6)$$

4. MODELING

4.a. Kinetic Model from Graaf et al. The kinetic model used to fit the experimental data was proposed by Graaf et al.[8−10] In a first study,[8] the authors performed calculations in order to characterize the chemical equilibrium in methanol synthesis. Thermodynamic equilibrium constants were calculated and are given in Table 6. In a second study,[9] methanol synthesis experiments were performed at low pressure (15−50 bar) and moderate temperature (210−245 °C) with a feed containing H_2, CO and CO_2 over a commercial $Cu/ZnO/Al_2O_3$ catalyst. Several mechanisms were studied assuming different rate-controlling steps, leading to 48 kinetic rate models. All reactions were assumed to be based on a dual-site Langmuir−Hinshelwood mechanism. One site was dedicated to the competitive adsorption of CO and CO_2, while the other site was devoted to the competitive adsorption of H_2 and H_2O. The adsorption of methanol was assumed to be negligible. One model was finally selected, thanks to an optimization procedure that minimized the differences between experimental and calculated data; the corresponding kinetic rate expressions for the methanol synthesis (reactions 1, 2, and 3) are given using eqs 7, 8, and 9:

Table 6. Equilibrium Constants (from Graaf et al.[8])

expression	comments
$\log_{10}(K_1) = \frac{5139}{T} - 12.621$	K_1 given in bar^{-2}; T given in K
$\log_{10}(K_2) = \frac{-2073}{T} - 2.029$	K_2 is dimensionless, T given in K
$\log_{10}(K_3) = \frac{3066}{T} - 10.592$	K_3 given in bar^{-2}, T given in K

DOI: 10.1021/acs.iecr.7b01323
Ind. Eng. Chem. Res. 2017, 56, 13133−13145

$$r_1 = k_1 b_{CO} \left\{ \frac{P_{CO} {P_{H_2}}^{3/2} - \frac{P_{CH_3OH}}{{P_{H_2}}^{1/2} K_1}}{(1 + b_{CO}P_{CO} + b_{CO_2}P_{CO_2})\left[{P_{H_2}}^{1/2} + \frac{b_{H_2O}}{{b_{H_2}}^{1/2}} P_{H_2O} \right]} \right\} \quad (7)$$

$$r_2 = k_2 b_{CO_2} \left\{ \frac{P_{CO_2} P_{H_2} - \frac{P_{CO} P_{H_2O}}{K_2}}{(1 + b_{CO}P_{CO} + b_{CO_2}P_{CO_2})\left[{P_{H_2}}^{1/2} + \left(\frac{b_{H_2O}}{{b_{H_2}}^{1/2}} \right) P_{H_2O} \right]} \right\} \quad (8)$$

$$r_3 = k_3 b_{CO_2} \left\{ \frac{P_{CO_2} {P_{H_2}}^{3/2} - \frac{P_{CH_3OH} P_{H_2O}}{{P_{H_2}}^{3/2} K_3}}{(1 + b_{CO}P_{CO} + b_{CO_2}P_{CO_2})\left[{P_{H_2}}^{1/2} + \left(\frac{b_{H_2O}}{{b_{H_2}}^{1/2}} \right) P_{H_2O} \right]} \right\} \quad (9)$$

where k_1 (in mol s^{-1} bar^{-1} kg_{cat}^{-1}), k_2 (in mol s^{-1} $bar^{-1/2}$ kg_{cat}^{-1}), and k_3 (in mol s^{-1} bar^{-1} kg_{cat}^{-1}) respectively represent the kinetic constants for reactions 1, 2, and 3; K_1, K_2, and K_3 are the equilibrium constants for each reaction (numerical values are given in Table 6); b_j corresponds to the adsorption constant of species j (numerical values are given in Table 7); and P_j represents the partial pressure of each species j.

Table 7. Adsorption Constants (from Graaf et al.[10])

expression	units
$b_{CO} = 2.16 \times 10^{-5} \exp\left(\frac{46800}{RT}\right)$	bar^{-1}
$b_{CO_2} = 7.05 \times 10^{-7} \exp\left(\frac{61700}{RT}\right)$	bar^{-1}
$\frac{b_{H_2O}}{{b_{H_2}}^{1/2}} = 6.37 \times 10^{-9} \exp\left(\frac{84000}{RT}\right)$	$bar^{-1/2}$

The numerical data provided in Table 6 are used in the calculations performed in the current work: indeed, the thermodynamic constants are dependent only on the temperature and remain unchanged when the feed conditions (pressure or composition for instance) and the catalyst are modified.

In a third study,[10] Graaf et al. characterized the influence of internal mass-transfer limitations in order to determine the intrinsic values of kinetic parameters. These numerical values are given in Table 8 and are dependent on the used catalyst, the operating conditions, and the hydrogen:carbon ratio. The pre-exponential factors and the activation energies are determined again in the current work to take into account the new working conditions and the new catalyst by minimizing the differences between experimental and modeling results. This work is described in the following section.

Table 8. Kinetic Constants (Graaf et al.[10])

expression	units
$k_1 = 4.89 \times 10^{7} \exp\left(\frac{-113\,000}{RT}\right)$	mol s^{-1} bar^{-1} kg_{cat}^{-1}
$k_2 = 9.64 \times 10^{11} \exp\left(\frac{-152\,900}{RT}\right)$	mol s^{-1} $bar^{-1/2}$ kg_{cat}^{-1}
$k_3 = 1.09 \times 10^{5} \exp\left(\frac{-87\,500}{RT}\right)$	mol s^{-1} bar^{-1} kg_{cat}^{-1}

4.b. Reactor Modeling. The reactor is represented with a pseudo-homogeneous perfect plug-flow model that has been developed with the following assumptions: isothermal conditions, steady-state regime, no axial dispersion, and no mass-transfer limitations.

Appendix B (in the Supporting Information) shows, in more detail, that all possible falsifying effects can be neglected. This leads to the pseudo-homogeneous one-dimensional model described for species j by a molar balance given by eq 10:

$$\frac{dF_j}{dm} = \sum_{i=1}^{n} \nu_{ij} r_i \quad (10)$$

where m denotes the catalyst mass, F_j the molar flow rate of species j, ν_{ij} the stoichiometric coefficient of species j in reaction i, and r_i the reaction rate of reaction i with respect to the catalyst mass. The pressure drops can be estimated in a fixed bed using the Ergun equation given in eq 11.

$$\frac{dP}{dm} = -\frac{1}{\rho_c(1-\varepsilon)\Omega}\left[\frac{150\mu_m(1-\varepsilon)^2 u}{\varepsilon^3 {d_p}^2} + \frac{1.75(1-\varepsilon)\rho_f u^2}{\varepsilon^3 d_p} \right] \quad (11)$$

with μ_m the dynamic viscosity of the fluid mixture, ρ_f its density, ε the void fraction of the catalytic bed, ρ_c the apparent catalyst density, Ω the reactor cross section, and u the superficial fluid velocity. The pressure drop was calculated for each experiment, and led to a value that was considered to be negligible (which was expected, given the short length of the reactor). The reactor can also be considered as isobaric.

4.c. Optimization Procedure. For the identification of kinetic parameters, the least-squares criterion, given by eq 12, has been chosen as the objective function to be minimized.

$$J = \sum_{k=1}^{n_{exp}} \sum_{j=1}^{m} (F_{k,j}^{model} - F_{k,j}^{exp})^2 \quad (12)$$

where $F_{k,j}^{exp}$ represents the experimental value of the molar flow rate of species j in experiment k and $F_{k,j}^{model}$ represents the one calculated by the numerical model based on the system of ordinary differential equations (eqs 10). The solver ode15s of Matlab software is used to solve this differential equation system.

The optimization procedure using Matlab is divided into two steps:

- A genetic algorithm was used to define boundaries corresponding to the parameters to be optimized,
- A gradient based optimization method to determine the optimum.

Confidence intervals with 15 degrees of freedom at a 95% significance level are provided for the determined pre-exponential factors and the energies of activation.

5. RESULTS

5.a. Thermodynamic Calculations. Expected compositions at thermodynamic equilibrium for all of the experimental scenarios were calculated with ProSim Plus software, using the Soave−Redlich−Kwong model, assuming an equilibrated flow reactor by minimizing the Gibbs free energy for a mixture of CO_2, CO, H_2, CH_3OH, and H_2O, as well as with N_2 and Ar as inerts. Detailed analysis of thermodynamic calculations is presented elsewhere.[23] In summary, it was found that CO_2 hydrogenation

DOI: 10.1021/acs.iecr.7b01323
Ind. Eng. Chem. Res. 2017, 56, 13133−13145

into methanol is favored at low reaction temperatures, high total pressure, and high hydrogen inlet partial pressure.

5.b. Identification of Kinetic Parameters. In the present paragraph, the optimization procedure previously described is used to identify some parameters appearing in eqs 7, 8, and 9. The same expressions of reaction rates as those obtained by Graaf et al.[9] are used: the catalysts used in the current work (CuZA or CuZZ) are similar to the catalyst used by Graaf et al., meaning that the adsorption mechanisms are close. Nevertheless, the experimental conditions are not analogous which justify new parameters identification. Indeed, in the present work, no carbon monoxide is introduced in the feed (contrary to the studies of Graaf et al.), the pressure range is higher (pressures of 50−80 bar) and the temperature conditions are different (temperature between 200 and 230 °C). The gas hourly space velocity ($GHSV_0$), calculated under standard conditions (T_0 = 0 °C, P_0 = 1 atm), is between 7800 and 23 400 h^{-1}. The $GHSV_0$ value, whose expression is given in eq 13, is defined as the ratio between the volumetric flow rate under standard conditions and the catalyst volume:

$$GHSV_0 = \frac{\rho_c(1-\varepsilon)Q_{v,0}}{m_c} \tag{13}$$

where ρ_c is the apparent density of the catalyst, ε the bed porosity, $Q_{v,0}$ the volumetric flow rate under standard conditions, and m_c the mass of catalyst.

In a first series of simulations, 12 parameters are estimated: 6 pre-exponential factors (3 related to kinetic constants and 3 related to adsorption constants), 3 activation energies, and 3 heats of adsorption. Although a correct representation of experimental points is performed, the obtained reaction rate constants calculated at 210 °C are very different from those obtained by Graaf et al. Moreover, the confidence interval obtained for each regressed parameter shows that the results are not relevant, from a statistical point of view; this is confirmed by the relatively weak number of experiments (17 for CuZA and 10 for CuZZ), compared to the number of researched parameters (12). Since the active phase of the catalyst is similar, the decision was made to use the adsorption constants determined by Graaf et al. in the optimization procedure. The considered expressions, as a function of temperature, are given in Table 7.

In a second series of simulations, 6 parameters are estimated: 3 pre-exponential factors related to kinetic constants and 3 activation energies. In this case, the reaction rate constant of reaction 1, concerning CO hydrogenation, is entirely negligible at 210 °C (a value on the order of 10^{-19} mol s^{-1} kg^{-1} bar^{-1} for CuZA is obtained), which is an expected result, given that the feed does not contain carbon monoxide in the experiments, leading to the fact that information is insufficient to properly identify the corresponding parameters. The decision was made to use the numerical value obtained by Graaf et al.[10] for the kinetic constant of reaction 1 in the reactor model.

Finally, 4 parameters are estimated: 2 pre-exponential factors related to the kinetic constants and 2 activation energies for reactions 2 and 3. The numerical results for the CuZA catalyst are given in Table 9.

A comparison between Table 8 (Graaf's results using a feed with a $CO/CO_2/H_2$ mixture) and Table 9 (results of the present study using a feed with a pure CO_2/H_2 mixture) shows that the numerical values are in the same order of magnitude for the reverse water-gas-shift reaction (reaction 2). Concerning the CO_2 hydrogenation (reaction 3), the pre-exponential factors and the energies of activation are very different. Despite these differences, a calculation of the reaction rate constant by the Arrhenius law at 210 °C shows that these values are similar (in the work of Graaf et al., k_3 (210 °C) = 3.78 × 10^{-5} mol s^{-1} kg^{-1} bar^{-1}; in the present work, k_3 (210 °C) = 4.85 × 10^{-5} mol s^{-1} kg^{-1} bar^{-1}). A series of parity plots, represented in Figure 1a, shows the good agreement between the experimental molar flow rates and the ones calculated by the model. This assessment is especially true for the molar flow rate of CO_2 and H_2. The difference between the model and the experiments is more important for CO and methanol, especially at high temperature. Under these conditions, the gap can be explained by the fact that the regime is close to the thermodynamic equilibrium; viable data are then difficult to be obtained.

Table 9. Optimized Kinetic Parameters for Reactions 2 and 3 for the CuZA Catalyst

reaction	pre-exponential factor (mol s^{-1} bar^{-1} kg_{cat}^{-1})	activation energy (J/mol)
2	(4.84 ± 0.3) × 10^{11}	140 020 ± 434
3	23.4 ± 0.2	52 570 ± 136

The sensitivity of the results has been tested by cancelling the reaction of CO hydrogenation (reaction 1) in the reactor model and by changing the objective function, respectively. An optimization has also been performed by removing reaction 1 from the reactor model. Not surprisingly, when CO hydrogenation is not considered, the numerical values of the kinetic constants are different: the reaction rate constants at 210 °C for CO_2 hydrogenation and for RWGS are slightly higher than those obtained by considering reaction 1 in the reactor model (relative deviations of 1.5% and 1.25% are respectively observed), which was expected because the methanol can be produced only by CO_2 hydrogenation. In both cases, the value of the objective function is similar and the agreement between experimental points and the model is not better. Consequently, all results presented in the article take into account reactions 1, 2, and 3 in the reactor model. A modified objective function, taking into account relative deviations, has been tested (the results are not presented in the article). While the results for the CO_2 and H_2 molar flow rates do not show any significant change, the agreement between experimental points and the model is slightly worse than that previously observed for the CO molar flow rate, especially for the higher temperatures. Concerning the methanol molar flow rate, the agreement is better at high temperature but worse at low temperature. Finally, since no significant improvement is observed, only the results corresponding to the objective function with absolute deviation are presented.

The same procedure has been applied for the CuZZ catalyst. The numerical results for this catalyst are given in Table 10. As the number of experiments decreases, the confidence intervals become wider for the CuZZ catalyst than for the CuZA one.

A series of parity plots for the CuZZ catalyst, represented in Figure 1b, shows the good agreement between the experimental molar flow rates and the ones calculated by the model. Concerning the quality of the results, a similar reasoning to that performed previously for the CuZA can be applied here for the CuZZ catalyst.

The analysis of the catalytic results presented in Tables 4 and 5 was done in terms of total pressure, temperature, hydrogen partial pressure, and GHSV variations. The influence of these parameters is described in the next paragraphs, especially for the CuZA catalyst.

DOI: 10.1021/acs.iecr.7b01323
Ind. Eng. Chem. Res. 2017, 56, 13133−13145

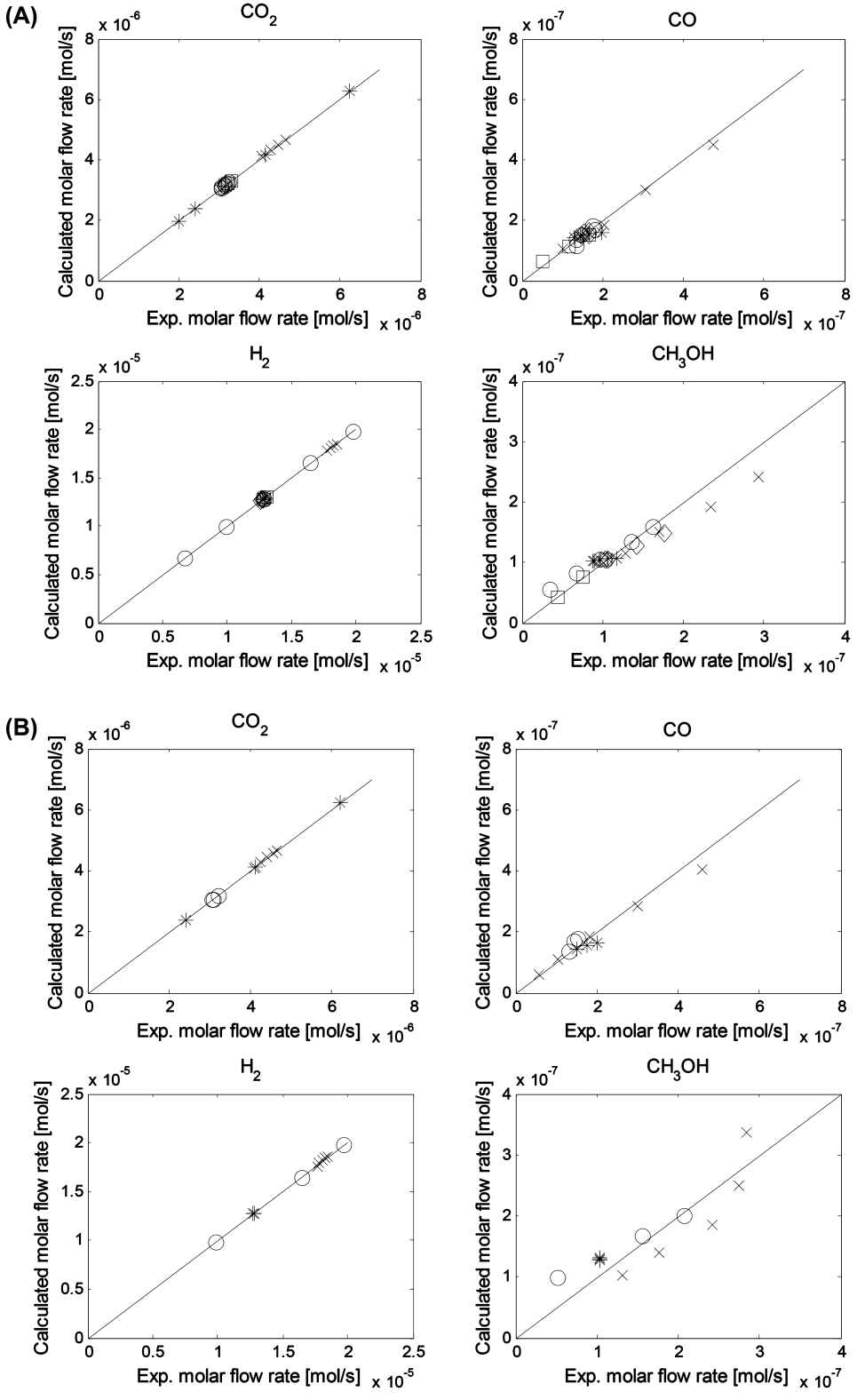

Figure 1. (a) Parity plots for the four-parameter optimization procedure for (a) the CuZA catalyst and (b) the CuZZ catalyst. (Legend: (×) *T* variation, (○) y_{H_2} variation, (*) y_{CO_2} variation, (◇) *P* variation, (□) GHSV variation. Correspondence with experiments in Table 4: *T* variation, experiments A–D; y_{H_2} variation, experiments 1–5; y_{CO_2} variation, experiments 6–9; *P* variation, experiments 3a and 3b; and GHSV variation, experiments 3.1 and 3.2.)

5.c. Effect of Reactor Walls. As the CuZZ catalyst was mixed with SiC in order to obtain the same catalytic bed volume as in the case of the CuZA catalyst, an additional test with pure SiC loading was performed under the same operating conditions, including the reduction pretreatment step. No conversion of CO_2 and H_2 was observed, and, as a consequence, no liquid products were obtained nor CO in the reactor outgas was detected. This experiment demonstrates the absolute inertness of the reactor walls and inactivity of SiC in the CO_2 hydrogenation into methanol.

DOI: 10.1021/acs.iecr.7b01323
Ind. Eng. Chem. Res. 2017, 56, 13133–13145

Table 10. Optimized Kinetic Parameters for Reactions 2 and 3 for the CuZZ Catalyst

reaction	pre-exponential factor (mol s^{-1} bar^{-1} kg_{cat}^{-1})	activation energy (J mol^{-1})
2	$(1.53 \pm 0.17) \times 10^{10}$	129 000 ± 848
3	$(1.71 \pm 0.03) \times 10^{1}$	51 605 ± 285

5.d. Effect of Temperature. The reaction temperature is varied between 200 °C and 230 °C. Since the catalyst tests were carried out at low conversion (<15%) in order to get maximal information, the experimental conversion is far from the conversion at thermodynamic equilibrium. Consequently, in the kinetic limited regime, an increase in temperature leads to an increase in the production of methanol and also has a positive effect on CO_2 and H_2 conversion. The increase of the reaction rates is directly due to the influence of temperature by the way of the Arrhenius law. The formation of CO is also promoted when the temperature increases, because of the reverse water-gas-shift reaction. The results are illustrated in Figure 2 for the CuZA catalyst: the outlet molar flow rates of CO_2, CO, H_2, and CH_3OH are plotted as a function of the temperature; experimental points are represented by crosses and the model is represented by the continuous line. A relatively important deviation between experiments and simulations is observed for the methanol molar flow rate at high temperature (220 and 230 °C) which is partially due to experimental imprecision. The closeness of the thermodynamic equilibrium may also explain the deviation. With simulations and experiments performed on the CuZZ catalyst, a variation of temperature leads to a similar evolution of the molar flow rates (not presented here).

5.e. Effect of Total Pressure. The total pressure is varied between 50 bar and 80 bar. From a thermodynamic point of view, the pressure has no effect on the RWGS reaction while an increase in pressure leads to a higher production of methanol at equilibrium. Since these experimental points are obtained in the kinetic regime, an increase in the total pressure implies a better adsorption of H_2 and CO_2 on the catalyst, which leads to better conversion of CO_2 and H_2 and higher methanol production. The results are shown for the CuZA catalyst in Figure 3, where the outlet molar flow rates of CO_2, CO, H_2, and CH_3OH are plotted as a function of the total pressure; experimental points are represented by diamonds (◇) and the model corresponds to the continuous line.

5.f. Effect of Hydrogen Partial Pressure. The variation of hydrogen partial pressure between 12.7 bar and 37.5 bar, at a constant carbon dioxide pressure (equal to 6.2 bar), corresponds to a variation of the hydrogen:carbon dioxide ratio between 2 and 6. The results are presented in Figure 4 for the CuZA catalyst. The outlet molar flow rates of CO_2, CO, H_2, and CH_3OH are plotted as a function of the hydrogen partial pressure; experimental points are represented by circles and the model corresponds to the continuous line. An increase of the hydrogen:carbon dioxide ratio leads to an increase of the reaction rates of reactions 1, 2, and 3, because the partial pressure of hydrogen has a positive effect in the corresponding expressions (eqs 5, 6, and 7). The conversion of carbon dioxide is also increased through reactions 2 and 3. The production of methanol is also improved. As the carbon monoxide flow rate increases, it is possible to conclude that the RWGS reaction is kinetically faster than the CO hydrogenation. The evolution of the outlet hydrogen molar flow rate is linear with the inlet hydrogen partial pressure, which is directly due to the increase of hydrogen quantity at the inlet, because hydrogen conversion is quite unaffected (<4%).

5.g. Effect of GHSV. The effect of the gas hourly space velocity (GHSV), whose definition is given in eq 13, is described in this section. The GHSV is varied between 7500 h^{-1} and 25 000

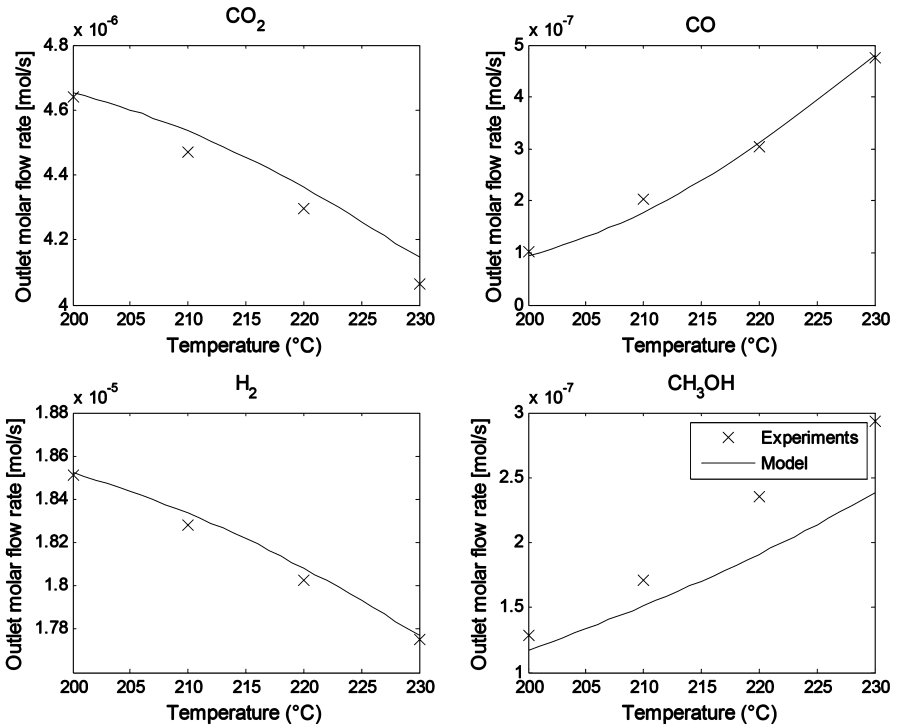

Figure 2. Molar flow rates of CO_2, CO, H_2, and CH_3OH, as a function of temperature on a CuZA catalyst at $GHSV_0$ = 7800 h^{-1}, P = 50 bar, H_2/CO_2 ratio = 3.9; the kinetic model from Graaf et al. and rate constants are given in Table 9.

DOI: 10.1021/acs.iecr.7b01323
Ind. Eng. Chem. Res. 2017, 56, 13133−13145

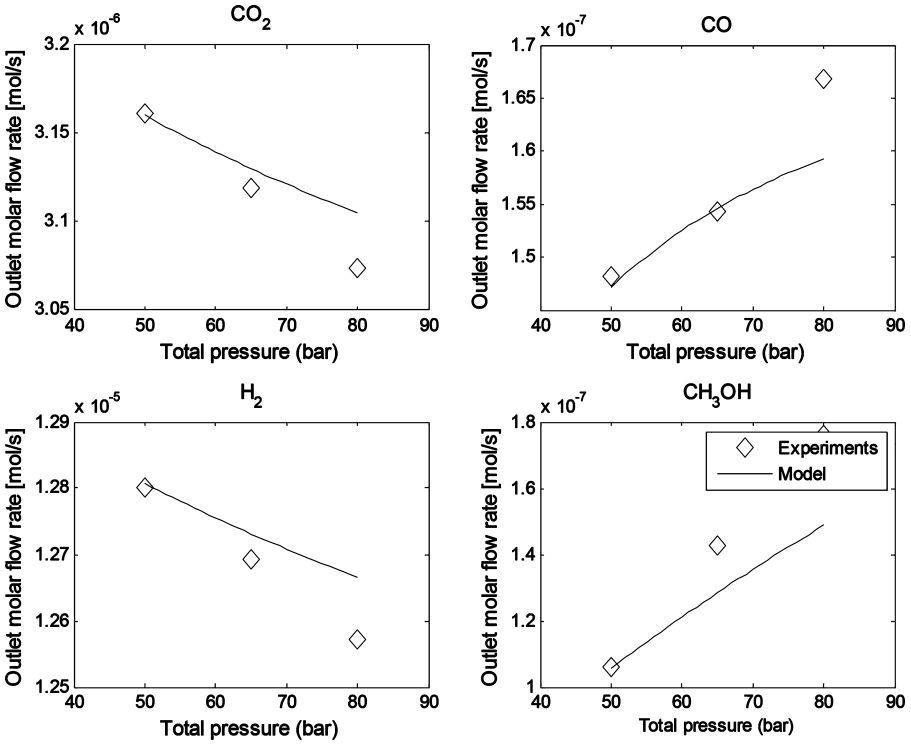

Figure 3. Molar flow rates of CO_2, CO, H_2, and CH_3OH, as a function of pressure on a CuZA catalyst at $GHSV_0 = 7800\ h^{-1}$, $T = 210\ °C$, H_2/CO_2 ratio = 3.9; the kinetic model from Graaf et al. and rate constants are given in Table 9.

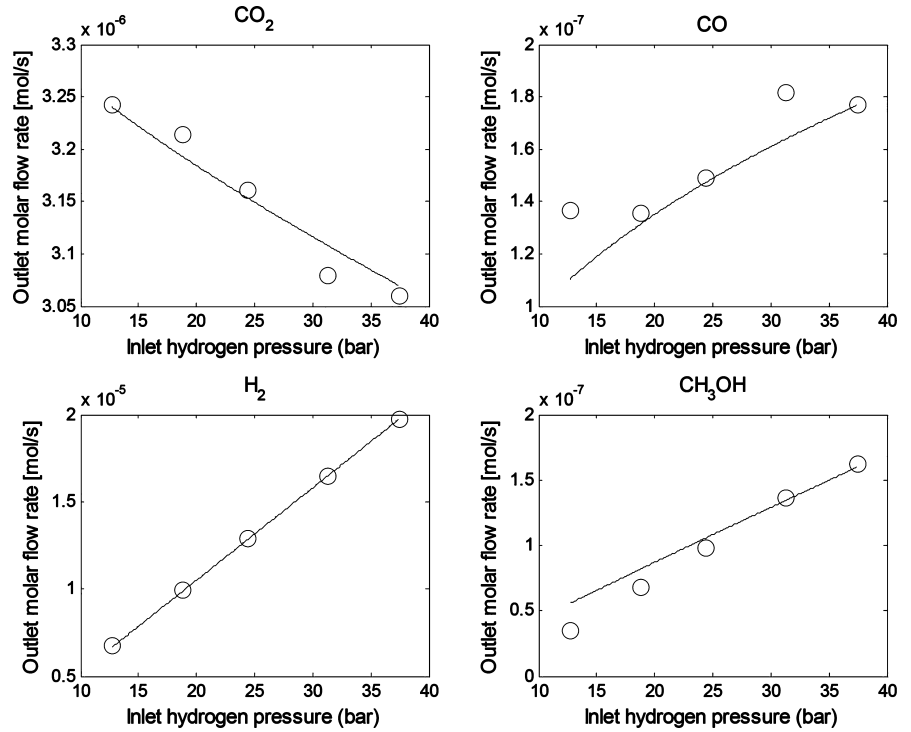

Figure 4. Molar flow rates of CO_2, CO, H_2, and CH_3OH, as a function of hydrogen partial pressure on a CuZA catalyst at $GHSV_0 = 7800\ h^{-1}$, $P = 50$ bar, $T = 210\ °C$; the kinetic model from Graaf et al. and rate constants are given in Table 9.

h^{-1}. Qualitatively, this parameter can be seen as a nondimensional velocity or as an inverse quantity of the space time. Consequently, an increase of the GHSV leads to a decrease of the residence time in the experimental reactor. This effect is clearly illustrated in Figure 5, where the outlet molar flow rates of CO_2, CO, H_2, and CH_3OH are plotted as a function of the GHSV; experimental points are represented by squares and the model corresponds to the continuous line. An increase in the GHSV implies a decrease in methanol production.

5.h. Comparison of Both Catalysts. A comparison between Table 9 (optimized parameters for CuZA as a catalyst) and Table 10 (optimized parameters for CuZZ as a catalyst)

DOI: 10.1021/acs.iecr.7b01323
Ind. Eng. Chem. Res. 2017, 56, 13133−13145

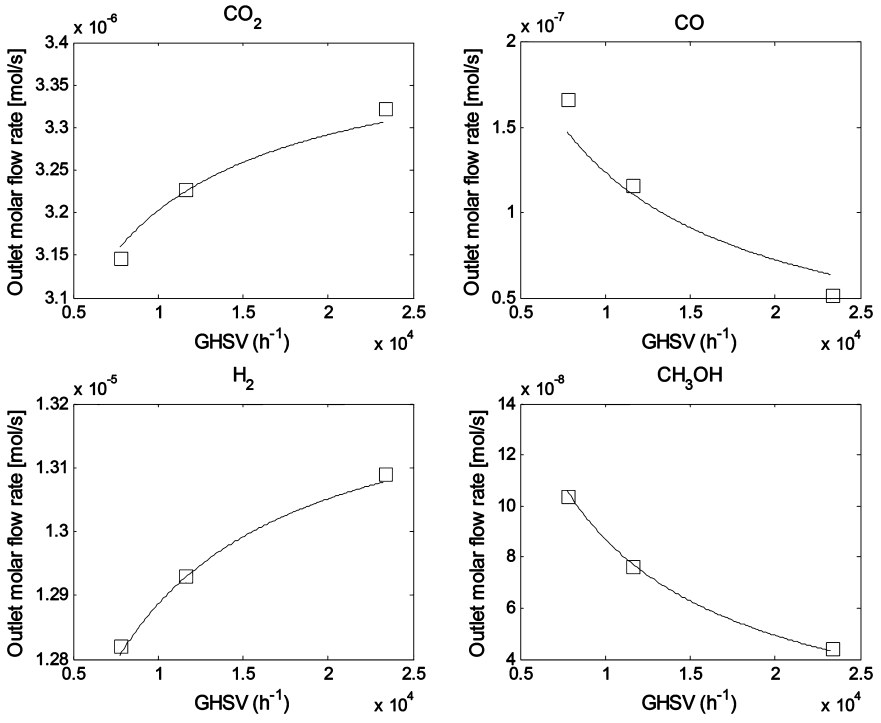

Figure 5. Molar flow rates of CO_2, CO, H_2, and CH_3OH, as a function of GHSV on a CuZA catalyst at P = 50 bar, T = 210 °C, H_2/CO_2 ratio = 3.9; the kinetic model from Graaf et al. and rate constants are given in Table 9.

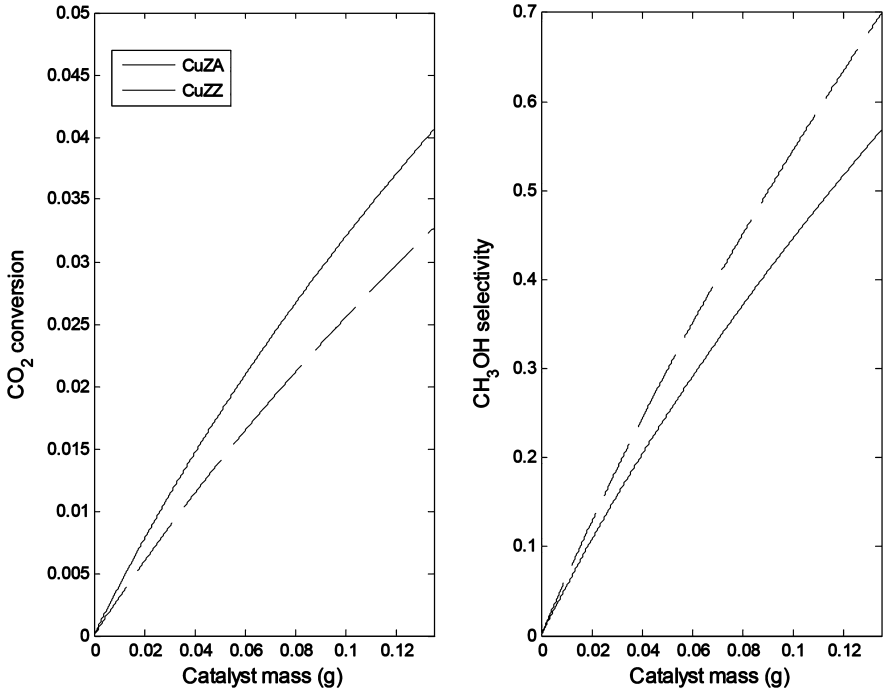

Figure 6. Carbon dioxide conversion and methanol selectivity for the CuZA and CuZZ catalysts (optimized model, $GHSV_0$ = 7800 h^{-1}, P = 50 bar, T = 200 °C, H_2/CO ratio = 3.9).

shows that the numerical values of the activation energies are slightly smaller in the presence of the CuZZ catalyst. The pre-exponential factors also differ. It is one order of magnitude smaller for the reverse water-gas-shift reaction (reaction 2), which indicates lower selectivity of the CuZZ catalyst toward CO formation during RWGS. Concerning the CO_2 hydrogenation (reaction 3), the pre-exponential factor is slightly smaller in the case of the CuZZ catalyst. Even though the results of characterization techniques of the CuZA material were slightly better than those for the CuZZ material (higher specific surface area and porosity, lower apparent density, more total porous volume), together with larger activation energy and similar pre-exponential factor, it may be concluded that the CuZZ catalyst, thanks to its support, shows a slightly decreased activity but improves the selectivity of methanol formation. This result is confirmed by simulating the experimental fixed bed with a

DOI: 10.1021/acs.iecr.7b01323
Ind. Eng. Chem. Res. 2017, 56, 13133−13145

pseudo-homogeneous model, taking into account the optimized kinetic parameters for both catalyst types. The comparison between the catalysts is performed in terms of carbon dioxide conversion and methanol selectivity and is given in Figure 6. If the CO_2 conversion is lower for the CuZZ catalyst, with respect to the CuZA catalyst, the methanol selectivity is higher confirming the catalyst characterization experiments.

6. CONCLUSION

In this work, the hydrogenation of carbon dioxide to methanol at high pressure has been tested on two noncommercial catalysts: a copper−zinc oxide catalyst on alumina (CuZA) and a copper−zinc oxide catalyst on zirconia (CuZZ). In this way, the influence of the catalyst support has been tested, showing that zirconia has a positive impact on methanol selectivity. Experiments have been performed (17 for the CuZA catalyst and 10 for the CuZZ one) in an isothermal fixed-bed reactor with a feedstock containing hydrogen, carbon dioxide, and inert compounds under different operating conditions (temperature range = 200−230 °C, total pressure range = 50−80 bar, GHSV range = 7800−23 400 h^{-1}, H_2/CO_2 molar ratio = 2−6). No carbon monoxide was present in the feed. A pseudo-homogeneous reactor model has been developed in order to identify kinetic parameters. The considered kinetic expressions for the reaction rates, based on a LHHW mechanism, are those established in a previous work by Graaf et al.[9] A new identification of the kinetic parameters for the methanol synthesis from a CO_2/H_2 mixture without CO addition was done. Although some mechanistic questions are still under discussion,[12] the results highlight good agreement between the experiments and the model in the considered range of operating conditions. Concerning carbon monoxide hydrogenation (reaction 1), the experiments did not allow one to properly calculate the kinetic constants (pre-exponential factor and activation energy), because no carbon monoxide was included in the feed. For the RWGS reaction (reaction 2), the determined kinetic constants are very similar to those obtained by Graaf et al., despite smaller activation energies. Finally, concerning the carbon dioxide hydrogenation (reaction 3), the pre-exponential factor and the activation energy are different, even if the reaction rate constant is similar to that calculated by Graaf et al. The hydrogen partial pressure has a positive effect on carbon dioxide conversion and methanol production. The interest of this study lies in the fact that the determined kinetic constants can be used to size a methanol synthesis reactor fed by a $CO_2/H_2/N_2$ mixture. As CO is produced in the reactor and can be recycled at the reactor inlet, the results are especially suitable in transient regime for the start-up phase when no CO is present.

■ ASSOCIATED CONTENT

Supporting Information

The Supporting Information is available free of charge on the ACS Publications website at DOI: 10.1021/acs.iecr.7b01323.

Appendix A shows experimental characterization of both catalysts. Appendix B shows assumptions made for the pseudo-homogeneous reactor model (PDF)

■ AUTHOR INFORMATION

Corresponding Author

*E-mail: jean-francois.portha@univ-lorraine.fr.

ORCID

Jean-François Portha: 0000-0001-8698-8635

Notes

The authors declare no competing financial interest.

■ ACKNOWLEDGMENTS

The authors thank the "Agence Nationale de la Recherche" (VItESSE2 project) for funding.

■ NOMENCLATURE

Latin Symbols

b_j = adsorption constant of component j
$C_{j,s}$ = molar concentration of component j at catalyst surface
C_j = molar concentration of component j in the bulk
$D_{m,j}$ = molecular diffusion coefficient of component j
$D_{eff,j}$ = effective diffusion coefficient of component j
d_p = diameter of catalyst particle
d_t = internal diameter of reactor
F_j = molar flow rate of component j
$f_{e,j}$ = external resistance fraction related to component j
K_i = equilibrium constant of reaction i
k_i = kinetic constant of reaction i
k_D = mass-transfer coefficient
L = reactor length
M = ratio of molar fractions at reactor inlet
m = mass of catalyst
m_c = total mass of catalyst in the reactor
n = partial reaction order
n_j = molar amount of component j
P = total pressure
P_j = partial pressure of component j
$Q_{v,0}$ = volumetric flow rate under standard conditions
R = ideal gas constant; R = 8.31 J/(mol K)
r_i = reaction rate of reaction i
S = selectivity
T = temperature
u = superficial velocity of the fluid
X = conversion
y_j = molar fraction of component j

Greek Symbols

ε = porosity of the bed
ε_p = porosity of the catalyst
μ_m = dynamic viscosity of the fluid mixture
ν_{ij} = stoichiometric coefficient of component j in reaction i
ρ_c = apparent catalyst density
τ_p = tortuosity of the catalyst
$\phi_{s,j}$ = Thiele modulus
Ω = reactor cross section

■ REFERENCES

(1) Olah, G. A. Beyond oil and gas: the methanol economy. *Angew. Chem., Int. Ed.* **2005**, *44*, 2636.

(2) Olah, G. A.; Goeppert, A.; Surya Prakash, G. K. Chemical recycling of carbon dioxide to methanol and dimethyl ether: from greenhouse gas to renewable, environmentally carbon neutral fuels and synthetic hydrocarbons. *J. Org. Chem.* **2009**, *74*, 487.

(3) Jadhav, S. G.; Vaidya, P. D.; Bhanage, B. M.; Joshi, J. B. Catalytic carbon dioxide hydrogenation to methanol: a review of recent studies. *Chem. Eng. Res. Des.* **2014**, *92*, 2557.

(4) Arab, S.; Commenge, J.-M.; Portha, J.-F.; Falk, L. Methanol synthesis from CO_2 and H_2 in multi-tubular fixed-bed reactor and multi-tubular reactor filled with monoliths. *Chem. Eng. Res. Des.* **2014**, *92*, 2598.

DOI: 10.1021/acs.iecr.7b01323
Ind. Eng. Chem. Res. 2017, 56, 13133−13145

(5) Luyben, W. L. Design and control of gas-phase reactor/recycle processes with reversible exothermic reactions. *Ind. Eng. Chem. Res.* **2000**, *39*, 1529.
(6) Arab, S. *Développement d'un procédé de synthèse de méthanol à partir de CO_2 et H_2*; Ph.D. Thesis; Université de Lorraine, Nancy, France, 2014.
(7) Pontzen, F.; Liebner, W.; Gronemann, V.; Rothaemel, M.; Ahlers, B. CO_2-based methanol and DME – Efficient technologies for industrial scale production. *Catal. Today* **2011**, *171*, 242.
(8) Graaf, G. H.; Sijtsema, P. J. J. M.; Stamhuis, E. J.; Joosten, G. E. H. Chemical equilibria in methanol synthesis. *Chem. Eng. Sci.* **1986**, *41*, 2883.
(9) Graaf, G. H.; Stamhuis, E. J.; Beenackers, A. A. C. M. Kinetics of low-pressure methanol synthesis. *Chem. Eng. Sci.* **1988**, *43*, 3185.
(10) Graaf, G. H.; Scholtens, H.; Stamhuis, E. J.; Beenackers, A. A. C. M. Intra-particle diffusion limitations in low-pressure methanol synthesis. *Chem. Eng. Sci.* **1990**, *45*, 773.
(11) Grabow, L. C.; Mavrikakis, M. Mechanism of methanol synthesis on Cu through CO2 and CO hydrogenation. *ACS Catal.* **2011**, *1*, 365.
(12) Kunkes, E. L.; Studt, F.; Abild-Pedersen, F.; Schlögl, R.; Behrens, M. Hydrogenation of CO2 to methanol and CO on $Cu/ZnO/Al_2O_3$: is there a common intermediate or not? *J. Catal.* **2015**, *328*, 43.
(13) Vanden Bussche, K. M.; Froment, G. F. A steady-state kinetic model for methanol synthesis and the water gas shift reaction on a commercial $Cu/ZnO/Al_2O_3$ catalyst. *J. Catal.* **1996**, *161*, 1.
(14) Park, N.; Park, M.-J.; Lee, Y. J.; Ha, K. S.; Jun, K. W. Kinetic modeling of methanol synthesis over commercial catalysts based on three-site adsorption. *Fuel Process. Technol.* **2014**, *125*, 139.
(15) Askgaard, T. S.; Norskov, J. K.; Ovesen, C. V.; Stoltze, P. A kinetic model of methanol synthesis. *J. Catal.* **1995**, *156*, 229.
(16) Ovesen, C. V.; Stoltze, P.; Norskov, J. K.; Campbell, C. T. A kinetic model of the water gas shift reaction. *J. Catal.* **1992**, *134*, 445.
(17) Skrzypek, J.; Lachowska, M.; Moroz, H. Kinetics of methanol synthesis over commercial copper/zinc oxide/alumina catalysts. *Chem. Eng. Sci.* **1991**, *46*, 2809.
(18) Villa, P.; Forzatti, P.; Buzzi-Ferraris, G.; Garone, G.; Pasquon, I. Synthesis of alcohols from carbon oxides and hydrogen. 1. Kinetics of the low pressure methanol synthesis. *Ind. Eng. Chem. Process Des. Dev.* **1985**, *24*, 12.
(19) Lee, J. S.; Lee, K. H.; Lee, S. Y.; Kim, Y. G. A comparative study of methanol synthesis from CO_2/H_2 and CO/H_2 over a $Cu/ZnO/Al_2O_3$ catalyst. *J. Catal.* **1993**, *144*, 414.
(20) Liu, X.-M.; Lu, G. Q.; Yan, Z.-F.; Beltramini, J. Recent advances in catalysts for methanol synthesis via hydrogenation of CO and CO_2. *Ind. Eng. Chem. Res.* **2003**, *42*, 6518.
(21) Angelo, L.; Kobl, K.; Tejada, L. M. M.; Zimmermann, Y.; Parkhomenko, K.; Roger, A.-C. Study of $CuZnMO_x$ oxides (M = Al, Zr, Ce, CeZr) for the catalytic hydrogenation of CO_2 into methanol. *C. R. Chim.* **2015**, *18*, 250.
(22) Chinchen, G. C.; Hay, C. M.; Vandervell, H. D.; Waugh, K. C. The measurement of copper surface areas by reactive frontal chromatography. *J. Catal.* **1987**, *103*, 79.
(23) Kobl, K.; Thomas, S.; Zimmermann, Y.; Parkhomenko, K.; Roger, A.-C. Power-law kinetics of methanol synthesis from carbon dioxide and hydrogen on copper-zinc oxide catalysts with alumina or zirconia supports. *Catal. Today* **2016**, *270*, 31.
(24) Kobl, K. *Aspects mécanistiques et cinétiques de la production catalytique de méthanol à partir de CO_2/H_2*, Ph.D. Thesis; Université de Strasbourg, Strasbourg, France, 2015.
(25) Taylor, R.; Krishna, R. *Multicomponent Mass Transfer*; Wiley Interscience: New-York, 1993.
(26) Villermaux, J. *Génie de la Réaction Chimique: Conception Et Fonctionnement Des Réacteurs*; Tec&Doc: Paris, 1993.
(27) Edwards, M. F.; Richardson, J. F. Gas dispersion in packed beds. *Chem. Eng. Sci.* **1968**, *23*, 109.
(28) Mears, D. E. The role of axial dispersion in trickle-flow laboratory reactors. *Chem. Eng. Sci.* **1971**, *26*, 1361.

DOI: 10.1021/acs.iecr.7b01323
Ind. Eng. Chem. Res. 2017, 56, 13133−13145